ENVIRONMENTAL RESEARCH
LETTERS

LETTER • OPEN ACCESS

Extreme cold events in Europe under a reduced AMOC

To cite this article: Virna L Meccia *et al* 2024 *Environ. Res. Lett.* **19** 014054

IOP Publishing Environ. Res. Lett. 19 (2024) 014054 https://doi.org/10.1088/1748-9326/ad14b0

ENVIRONMENTAL RESEARCH
LETTERS

LETTER

Extreme cold events in Europe under a reduced AMOC

Virna L Meccia[1,*], Claudia Simolo[1], Katinka Bellomo[2,3] and Susanna Corti[1]

[1] National Research Council, Institute of Atmospheric Sciences and Climate, Bologna, Italy
[2] Department of Environment, Land and Infrastructure Engineering, Polytechnic University of Turin, Turin, Italy
[3] National Research Council, Institute of Atmospheric Sciences and Climate, Turin, Italy
* Author to whom any correspondence should be addressed.

E-mail: v.meccia@isac.cnr.it

Keywords: EC-Earth3 climate model, AMOC weakening, cold spells, atmospheric blocking, jet stream

Supplementary material for this article is available online

OPEN ACCESS

RECEIVED
29 September 2023

REVISED
16 November 2023

ACCEPTED FOR PUBLICATION
12 December 2023

PUBLISHED
19 December 2023

Abstract

There is a consensus that a weakened Atlantic Meridional Overturning Circulation (AMOC) decreases mean surface temperature in the Northern Hemisphere, both over the ocean and the continents. However, the impacts of a reduced AMOC on cold extreme events have not yet been examined. We analyse the impacts of a reduced AMOC strength on extreme cold events over Europe using targeted sensitivity experiments with the EC-Earth3 climate model. Starting from a fully coupled ocean-atmosphere simulation in which the AMOC was artificially reduced, a set of atmosphere-only integrations with prescribed sea surface temperature and sea-ice cover was conducted to evaluate the effects of weakly and strongly reduced AMOC strength. Despite overall cooling, reduced AMOC leads to fewer winter cold spells in Europe. We find that the weakened AMOC intensifies near-surface meridional gradient temperature in the North Atlantic and Europe, thus providing the energy to boost the jet stream. A stronger jet stream leads to less atmospheric blocking, reducing the frequency of cold spells over Europe. Although limited to the output of one model, our results indicate that a reduced AMOC strength may play a role in shaping future climate change cold spells by modulating the strength of the jet stream and the frequency of atmospheric blocking.

1. Introduction

The atmosphere and the ocean work together to compensate for the differences in solar radiation between the low and high latitudes by transporting annually up to 5.7 PW of heat poleward [1]. This way, the anomalies in heat transported individually by the atmosphere and ocean should approximately balance one another, a process known as Bjerknes compensation [2]. In the northern hemisphere (NH), the Atlantic Meridional Overturning Circulation (AMOC) carries up to 25% of the northward global atmosphere-ocean heat transport [3], while the atmosphere is especially efficient in transporting heat poleward by storms at mid-latitudes (around 40° N). Therefore, if the ocean heat transport in the North Atlantic is reduced, for example, by a reduction of the AMOC, it could be expected that the atmosphere would become more efficient to compensate for the deficit in oceanic heat transport. The European weather and climate would be affected by such a scenario because it is strongly influenced by the North Atlantic variability. It is in Europe where the westerly jet stream and the North Atlantic storm track end, and the North Atlantic is a region prone to atmospheric blocking [4].

Despite global warming, the North Atlantic subpolar gyre presented a relative cooling of sea surface temperatures (SST) during the last decades, a feature that is more pronounced in the boreal winter [5]. The observed spatial pattern of the subpolar gyre cooling is consistent with a slowdown of the AMOC, causing a reduced northward ocean heat transport and a northward shift of the Gulf Stream [6]. Some studies demonstrate that a cold SST anomaly in the North Atlantic can cause changes in the atmospheric circulation over Europe (e.g. [7]). For example, such an anomaly can increase the meridional temperature gradient and, therefore, the baroclinic instability [8], from where the wave activity takes energy and can modify the North Atlantic storm track.

Therefore, in the future, we will likely be exposed to the direct effects of global warming and those of a reduced AMOC. To disentangle these two drivers, it is possible to artificially reduce the AMOC by the so-called water hosing experiments. These experiments consist of a release of freshwater into the North Atlantic to inhibit deep water formation associated with AMOC. The freshwater anomaly can be applied under the pre-industrial climate, so the effects of a reduced AMOC can be accounted for without considering global warming. By doing so, some authors analysed the climate impacts of a reduced AMOC (e.g. [9–12]), and most works agree that the North Atlantic cools, thus increasing the meridional temperature gradient. To compensate for this cooling, the Intertropical Convergence Zone shifts southward to allow for more heat transport across the equator (e.g. [9, 11, 13–15]). Other studies reported an increase in sea level along the North American Atlantic coast [16] or an increase in the strength of the boreal winter North Atlantic storm track penetrating farther into western Europe [11, 17].

More specifically, some works focus on the climate impact on Europe [18] reported lower temperatures, reduced precipitation, increased snow cover, and higher albedo. [11] found that the intensified storm activities increase rainfall locally in winter, whereas summer precipitation decreases in northern Europe and increases in southern Europe. [15] found an increase in the frequency of the North Atlantic Oscillation positive phase during winter, associated with more wet days over northern Europe and drier conditions over southern Europe.

However, the impacts of an AMOC weakening on extreme weather phenomena in Europe have not been studied yet. For instance, although it is already known that a weakening of the AMOC can produce colder mean temperatures to the North Atlantic, the effects on the frequency of extreme cold events are unknown. Indeed, cold spells, defined as prolonged periods of extremely cold weather, have damaging consequences for agriculture, power demand, human health, and infrastructure (e.g. [19–21]). This study aims to fill this gap by investigating the impacts of a reduced AMOC on extreme cold events in Europe through targeted sensitivity simulations with the EC-Earth3 climate model.

The paper is organised as follows. In the next section, we introduce the climate model and the set of simulations and describe the methods. We present the results regarding the extreme cold events and propose an explaining mechanism in section 3, whereas the discussion and conclusions are presented in section 4.

2. Methodology

2.1. Model experiments

The experiments were conducted with the CMIP6-generation EC-Earth3 climate model [22], developed by a consortium of European research institutes. EC-Earth3 is constituted by the Integrated Forecast System (IFS; [23]) cycle 36r4, including the land-surface scheme H-TESSEL [24], and the Nucleus for European Modelling of the Ocean (NEMO; [25]) version 3.6, including the Louvain la Neuve (LIM3; [26]) sea-ice model. Both components communicate through the OASIS3-MCT version 3.0 coupler [27]. We use the model in its standard configuration: the T255L91 for IFS, which implies a horizontal resolution of ∼80 km and 91 vertical levels in a hybrid coordinate system, and ORCA1Z75 for NEMO, a tripolar grid with an average resolution of 1 degree and 75 vertical levels.

Following the protocol for the North Atlantic Hosing Model Intercomparison Project [28], a water hosing strength of 0.3 Sv (1 Sv $= 10^6$ m^3 s^{-1}) was uniformly distributed poleward of 50° N in the Atlantic and Arctic Oceans for 140 years to the pre-industrial climate. As a result, the AMOC reduces (figure S1). This experiment is documented in [15] where it was used to investigate the impacts of a weakened AMOC on precipitation patterns over the Euro-Atlantic sector. For more details on this experiment, the reader is thus referred to [15].

We used the above-described fully coupled ocean-atmosphere simulation to provide the initial conditions (ICs) and boundary conditions (BCs) for a series of Atmospheric Model Intercomparison Project (AMIP)-like experiments, in which the SST and sea-ice cover are prescribed. The purpose of these experiments is to investigate the changes in European extreme cold events in response to different levels of AMOC weakening. We selected three periods of 11 year duration in which the mean AMOC strength is about 17.5 Sv, 14 Sv and 7 Sv, respectively (figure S1). For each of the three periods, we used the atmospheric ICs and the simulated monthly SST and sea-ice cover as BCs (figure S2) for the AMIP-like runs. Thus, the set of experiments consists of a control run (*ctrl;* mean AMOC ∼17.5 Sv), a weak (−20% with respect to the control) AMOC reduction (*a14*; mean AMOC ∼14 Sv), and a strong (−60% with respect to the control) AMOC reduction (*a07*, mean AMOC ∼7 Sv).

By perturbing the 3D temperature field in the atmospheric component we generated 20 ensemble members for each of the 11 year long set of experiments. This strategy allows for a better disentanglement between internal and forced variability when looking at the ensemble means. In this case, the forcing is given by the level of AMOC reduction (0%, −20%, and −60%, approximately). Besides, this strategy allows to increase the amount of data by a factor of 20 and the statistical robustness, particularly when studying extreme or rare events. We considered the first year as a spin-up period to let the model adjust to the IC. Therefore, all the analysis performed in this study is made using 10 years of each

Table 1. Acronyms related to the minimum temperature used in this study.

Acronyms	Full name
Tasmin or *TN*	Minimum near-surface air temperature
TNm	Mean value of TN
TNn	Minimum value of TN
TNstd	Standard Deviation of TN
CSDI	Cold Spell Duration Index

simulation. We concatenate the monthly and daily outputs from these 3 experiments, each consisting of 10 year long 20 ensemble members, thus covering 200 years of data.

2.2. Methods

We used daily minimum near-surface air temperature (*tasmin* or *TN*) from model simulations to investigate changes in the severity and duration of cold-season cold extremes with the AMOC decline. Specifically, we analysed changes in the winter mean (*TNm*) and minimum (the coldest night *TNn*) of *TN* and in the Cold Spell Duration Index (CSDI, see table 1 for acronyms). The CSDI is the count of days with at least six consecutive days when the *TN* falls below the 10th percentile in the calendar five day window [29]. We compute the five day window 10th percentile of *TN* for each of the three experiments separately. These values represent the threshold for calculating the CSDI. Then, for the 200 year data of each experiment, we counted the days belonging to a cold spell (at least six consecutive days when the *TN* is lower than the threshold for that calendar day). This computation is done for the boreal winter season (December–January–February, DJF).

Atmospheric blocking, which is characterized by a stationary anomaly that blocks the prevailing westerlies winds, is computed with the tool Mid Latitude Evaluation System Version v0.51 [30]; using the daily geopotential height fields at 500 hPa (*zg500*) in a 2.5° × 2.5° grid. The tool calculates the two-dimensional blocking index or percentage of blocked days based on the reversal of the meridional gradient of *zg500* in the 30° N to 75° N latitude range [31].

The jet stream daily indices are computed based on the daily zonal wind at 850 hPa (*ua850*), according to [32]. The method consists of zonally averaging the zonal wind over the sector 0°–60° W between 15° N and 75° N. Then, the maximum value (westerly wind) is identified after applying a ten day low-pass filter. The latitude and value of this maximum are used to define the daily jet latitude and speed, respectively.

When plotting the differences between experiments, we present the results with a measure of agreement. Stippling indicates where more than 75% of the ensemble members have the same sign of difference as the ensemble mean, indicating that the signal is robust.

3. Results

3.1. Statistics of daily minimum near-surface temperature

Because the AMOC transports heat northward towards the high latitudes of the NH, the effect of a reduced AMOC is a widespread cooling of the NH, particularly in the North Atlantic sector (figures 1(a)–(c)), in agreement with previous studies (e.g. [11, 15]). This response is intensified during boreal winter [33] when the deep convection is inhibited. The strongest cooling is located around 70° N. As a result, the mean meridional temperature gradient increases (i.e., reinforces) south of 70° N and decreases north of 70° N (figures 1(d)–(f)). Overall, this can be interpreted as a southward shift of the maximum meridional gradient with the AMOC weakening. Blue shading in figure 1(d) indicates that the meridional temperature gradient is negative (reduction of temperature when latitude increases) in the control. Blue shading in figures 1(e) and (f) indicates a more negative meridional temperature gradient or intensification of it when the AMOC is reduced with respect to the control.

We focus now on the daily minimum temperature (*tasmin* or *TN*) in Europe (35° N to 70° N and 10° W to 40° E) over land during DJF. The regional mean minimum temperatures (*TNm*) show a decrease of about 2.5 °C and 7.2 °C relative to the control in the *a14* and the *a07* experiments, respectively (figures 2(a) and (b)). However, the minimum values of *TN* (*TNn*) decrease faster than the mean *TNm* (figures 2(b) and (d)) because of a concurrent increase in *TN* standard deviation (*TNsd*, figure 2(b)) that accelerates the cooling of the coldest nights (see e.g. [34]). The difference in the standard deviation is 0.5 and 1.3 °C for the *a14* and *a07* experiments, respectively. The spatial patterns of *TNsd* and the differences between *TNn* and *TNm* are shown in figure S3. The increase in variability is widespread (figures S3(a) and (b)) and largely explains the excess cooling of *TNn* over much of the NH (figures S3(c) and (d)). In turn, changes in temperature variability with the AMOC decline are likely related to changes in the mean meridional gradient, as their pattern similarities may suggest (figures 1(e) and (f) vs figures S3(a) and (b)). Namely, variability tends to increase where the gradient strengthens, as already found in global warming projections [34–36].

In summary, from the statistical distributions of the daily minimum near-surface air temperature over Europe, an AMOC weakening yields a cooler winter climate with increased variability in which the coldest nights are expected to become more extreme. We will

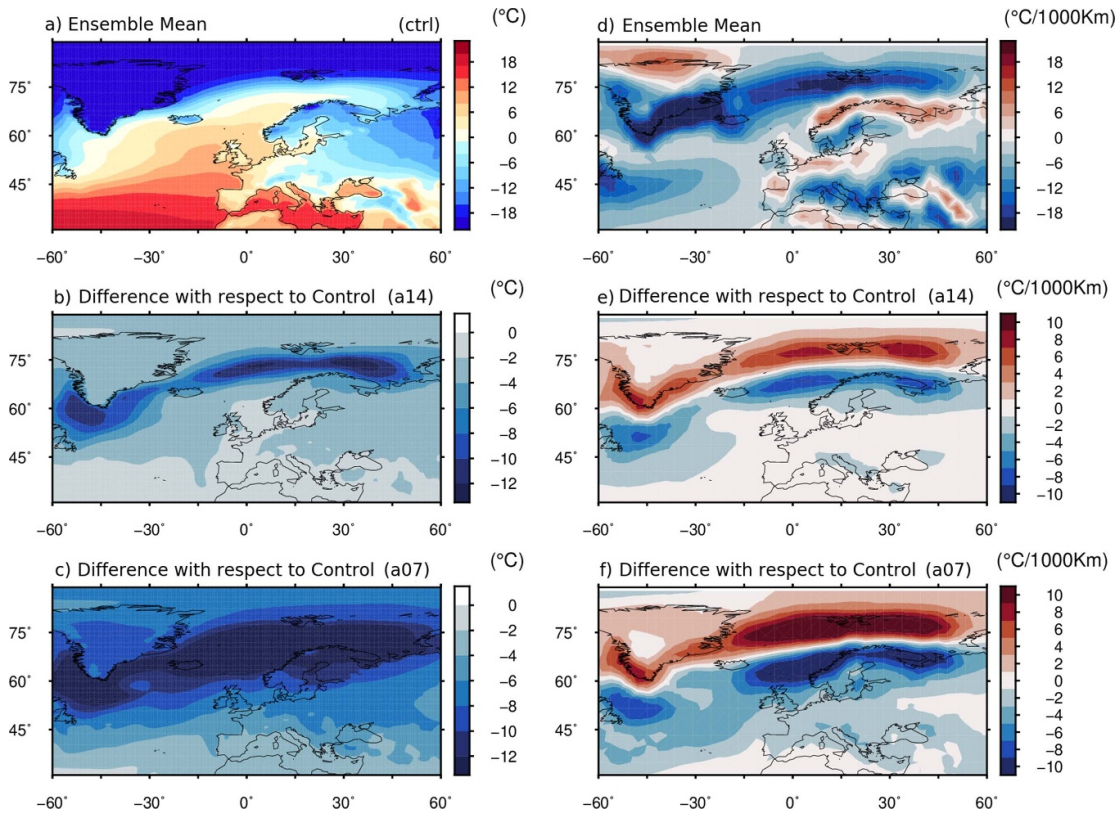

Figure 1. (a), (b) and (c) boreal winter (DJF) mean near-surface air temperature (*tas*; °C) in the North Atlantic and Europe. The ensemble mean for the *ctrl* is plotted in (a), and the anomalies of *a14* and *a07* with respect to the control are plotted in (b) and (c), respectively. (d), (e) and (f) Boreal winter mean near-surface air temperature meridional gradient (°C/1000 Km) in the North Atlantic and Europe. The ensemble mean for the *ctrl* is plotted in (d), and the anomalies of *a14* and *a07* with respect to the control are plotted in (e) and (f), respectively.

now investigate how these extremely cold temperatures aggregate throughout the winter.

3.2. The cold spells in Europe

We computed the CSDI for DJF in each grid point for the three sets of experiments independently. Figure 3(a) show the ensemble mean of the mean CSDI per winter (averaged over the total number of years) over land for the *ctrl* run. If the CSDI is less than 6 days, that means that less than one event per winter, on average, occurs. The differences of the ensemble mean of CSDI for *a14* and *a07* with respect to *ctrl* are plotted in figure 3(b) and (c), where red shading indicates more days while blue shading indicates fewer days belonging to a cold spell with respect to the control. Similarly, figure S4 shows the mean frequency and duration of cold spells per winter. In the case of a weak reduction of the AMOC (*a14*), the internal variability is larger than the forced signal, and the results are not robust. Yet, some features resemble those obtained in the case of a strong AMOC reduction (*a07*) in which the ensemble mean signal is in agreement with more than 75% of the ensemble members. For instance, although cooler mean winters occur with a reduced AMOC (figures 1(b) and (c)), there are areas in which the number of days belonging to cold spells decreases. The latter occurs in central Europe, Ireland, the southern UK, and Eastern Europe (figure 3(c)). A moderate (not robust) increase in the CSDI is found in Scandinavia, the northern UK, and southern Europe.

We focus now on the two areas enclosed by the black boxes in figure 3(c), where the CSDI is reduced due to an AMOC weakening, in central Europe, Ireland and the southern UK (A1), and Eastern Europe (A2). We identified the cold spell events in each grid point of areas A1 and A2, separately. By summing up all the events, we constructed the histograms of the duration in days of cold spells in each area for the three experiments (figure 4). In both regions, the frequency of cold spells decreases when the AMOC is reduced, and this is true for almost all the durations. The longest cold spell duration in A2 decreases from 14 to 11 days in the case of a strong AMOC reduction. In summary, even though a reduced AMOC leads to cooler mean winters, the extremely cold days are less aggregated, and consequently, fewer days are associated with cold spell events.

To explore the atmospheric conditions associated with extreme cold events in regions A1 and A2, we computed the composites of geopotential height anomalies at 500 hPa (*zg500*) for the days belonging to a cold spell in the selected areas. To do so, we first

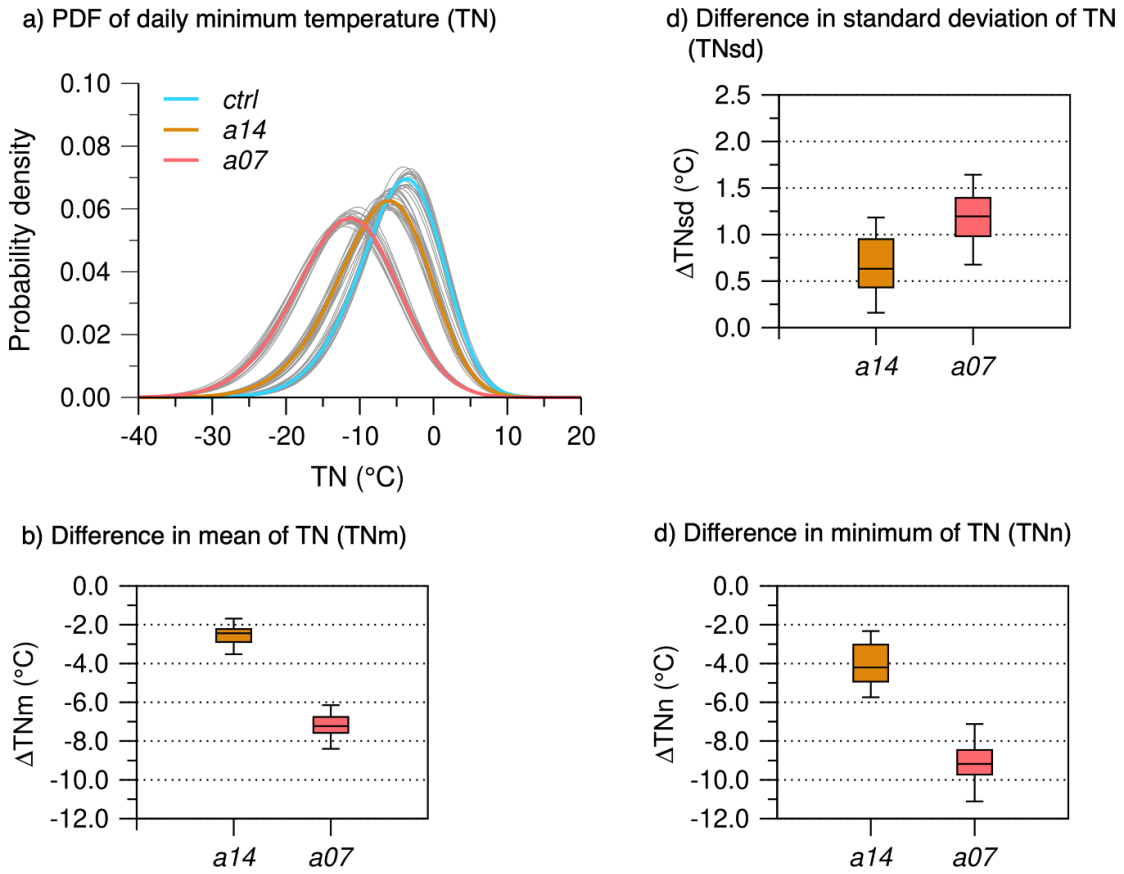

Figure 2. Statistics for the boreal winter daily *tasmin* or *TN* in Europe over land: (a) probability density functions; (b); (c); and (d) boxplots for the differences in the mean; standard deviation; and minimum, respectively for the experiments with a reduced AMOC with respect to the control.

recomputed the CSDI for the areal mean *TN* to obtain a single index per area to calculate the composites. The resulting fields for the control experiments are plotted in figure 5(a) for A1 and figure 5(b) for A2. Results for the experiments with the reduced AMOC are similar to those of the control (figure S4); the anomalies are independently computed for each set of experiments based on the daily climatology. In all three cases, the *zg500* anomaly field associated with cold spells in both areas A1 and A2 resembles the pattern of the North Atlantic atmospheric blocking [37–39] in which a positive anomaly develops over Scandinavia and the Nordic seas and a negative anomaly develops over southern Europe. Then, because the cold spells in A1 and A2 are associated with atmospheric blocking in the North Atlantic, we will explore the response of this phenomenon to a reduction of the AMOC in the following section.

3.3. The North Atlantic atmospheric blocking

The ensemble mean of the mean frequency of blocked days in boreal winter for the *ctrl* run is plotted in figure 6(a). The differences of the ensemble mean for *a14* and *a07* with respect to *ctrl* are plotted in figures 6(b) and (c), where red shading indicates more blocked days and blue shading represents fewer blocked days with respect to the control. In both experiments with a reduced AMOC, the number of blocked days per winter is reduced in the North Atlantic, Nordic seas, and Greenland. Although this signal is weak in the *a14* experiments, the response is stronger when the AMOC weakening is stronger, too. The reduction of the blocked days for the *a07* experiments is more intense, robust, and widespread, resulting in fewer blocked days also over the mid-latitudes North Atlantic, Scandinavia and the UK. Blockings have increased south of 40° N. However, these blocking-like structures are oscillations in the subtropical high-pressure systems [31] and are unable to block or divert the atmospheric flow. Therefore they have a negligible impact on weather patterns.

So far, we have found that the cold spell events in central and Eastern Europe are associated with a *zg500* blocking pattern. We also found that less North Atlantic atmospheric blocking occurs in a climate with a reduced AMOC, which could explain why counting days belonging to extreme cold events in A1 and A2 is also reduced. Atmospheric blocking can be described as a weather pattern in which the prevailing westerly winds are blocked by a persistent and stationary anomaly, generally an anticyclone. Therefore, blocking systems often occur in regions

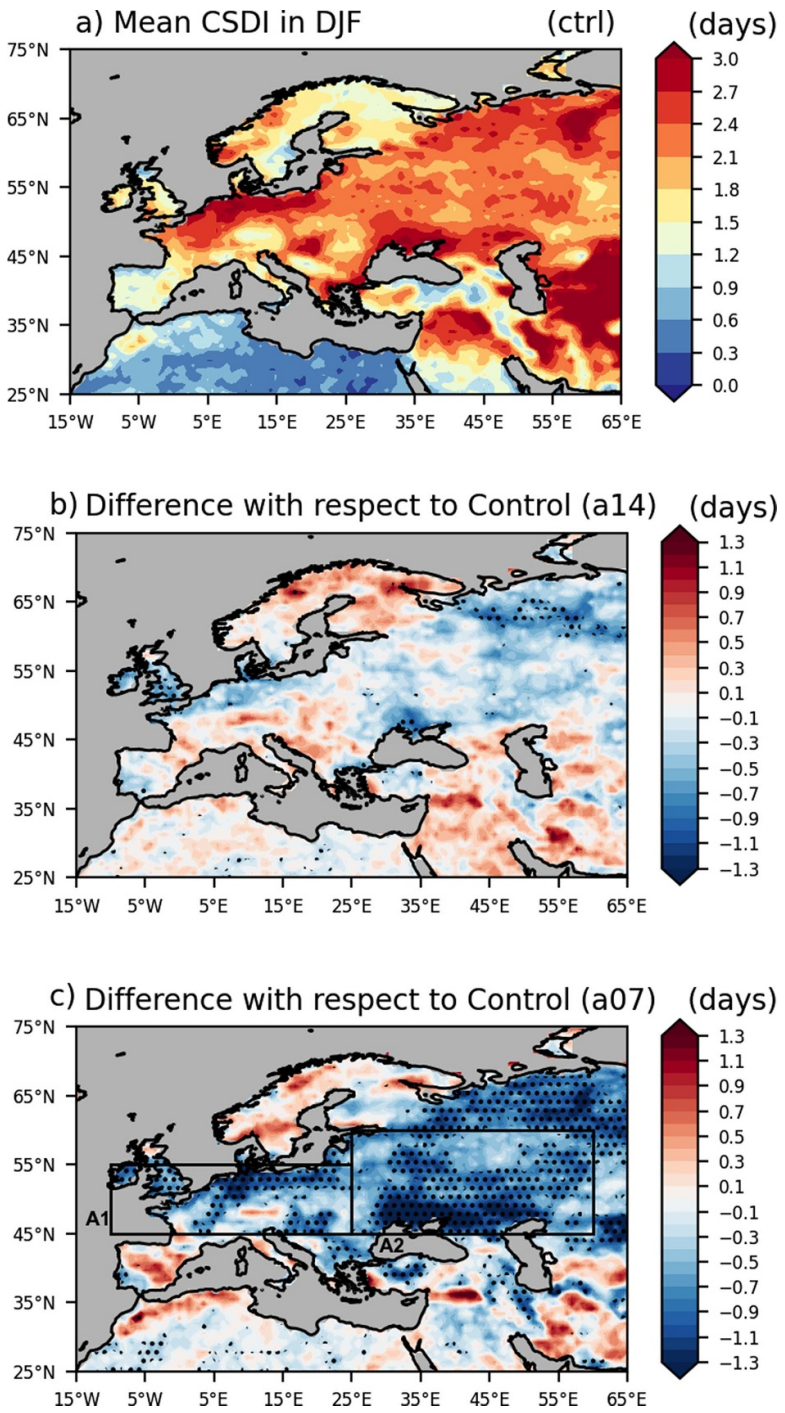

Figure 3. Cold spell duration index for DJF. (a) shows the ensemble mean of the mean number of days per winter belonging to a cold spell for the *ctrl* experiments. (b) and (c) show the difference with respect to the control run. Dots in (b) and (c) are plotted when more than 75% of the ensemble members have the same sign of difference as the ensemble mean.

of weak flow with a lower wave propagation capacity [40]. To explain the relation between the frequency of blocked days in winter and the AMOC strength, we explore the response of the jet stream to a reduced AMOC in the next section.

3.4. The jet stream

The zonal mean of the zonal wind in DJF is plotted as a function of latitude and height for the control experiments in figure 7(a). Results for *a14* and *a07* are plotted as differences with respect to the control in figures 7(b) and (c). In addition, figures 7(d) and (e) show the daily jet latitude and speed indices computed as explained in section 2.2. In a climate with a weaker AMOC, the PDF of the jet latitude index (figure 7(d)) exhibits an enhanced frequency in the central peak at around 45° N. This feature is very noticeable in the case of a strong reduction of the AMOC and softer, though still present, in the case of a weak AMOC reduction. In addition,

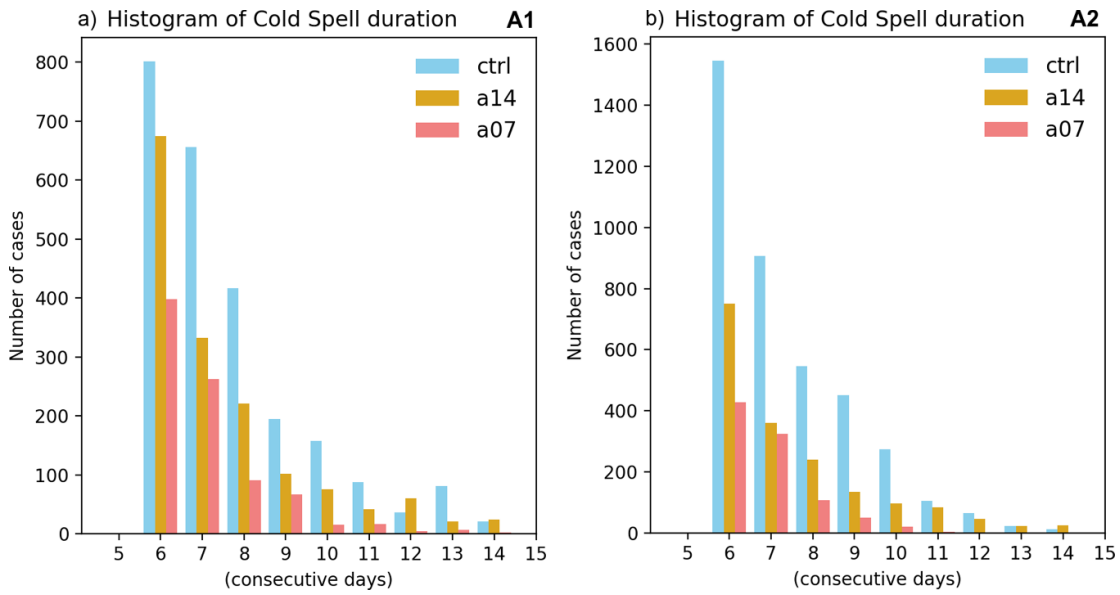

Figure 4. Histograms of the cold spell duration in days for the three sets of experiments in (a) A1 and (b) A2, as indicated with the black boxes in figure 3(c). The cold spells in each grid point of A1 and A2 are summed up separately.

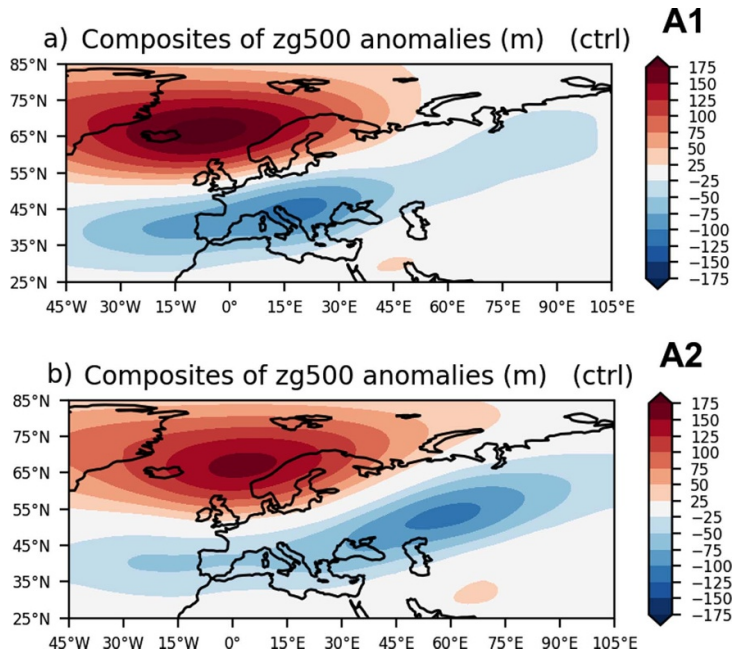

Figure 5. Composites of geopotential height anomalies at 500 hPa (m) for days belonging to cold spell events in the mean areal (a) A1 and (b) A2 for the *ctrl* experiment.

the jet stream speed is larger in the cases of a weaker AMOC (figures 7(c) and (e)). Indeed, the mean value in each distribution is 13.6, 13.9, and 14.7 m s^{-1} for the *ctrl*, *a14*, and *a07* experiments, respectively.

Since an AMOC weakening leads to a mean cooling in the high latitudes of the North Atlantic, the meridional gradient of temperature increases. The intensified temperature gradient results in a stronger jet stream, which more easily inhibits the formation of blocking systems.

4. Discussion and conclusions

We have performed a series of AMIP-like experiments with the EC-Earth3 climate model, intending to study the relation between the AMOC strength and the extreme cold events in Europe. With this purpose, we have analysed three sets of experiments, each one consisting of 10 year long 20 ensemble members. The AMOC was artificially weakened by applying water hosing to the North Atlantic and the Arctic in a coupled run. Then, we used three time slices of

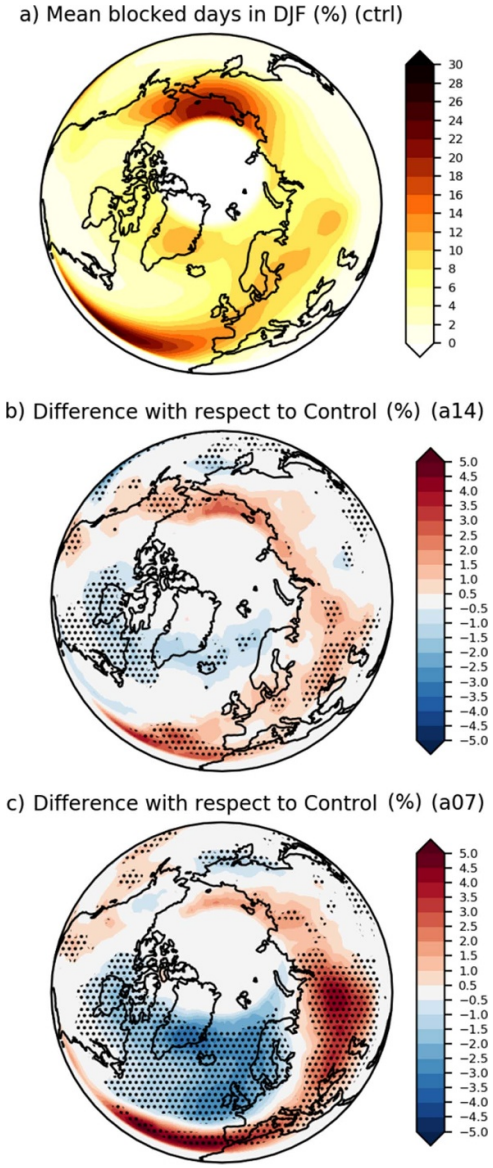

Figure 6. 2D blocking index for DJF. (a) the ensemble mean of the frequency of blocked days for the *ctrl* experiment, (b) and (c) difference of *a14* and *a07* with respect to the *ctrl*. Dots in (b) and (c) are plotted when more than 75% of the ensemble members have the same sign of difference as the ensemble mean.

this simulation with different levels of AMOC weakening (0%, −20% and −60%) to provide the ICs and BCs for the AMIP-like experiments. The first set of experiments (*ctrl*) uses the IC and BC from the CMIP6 *piControl* run and represents a climate with a mean AMOC strength of ∼17.5 Sv. The second (*a14*) and third (*a07*) sets of experiments use the ICs and BCs reached through the water hosing simulation, representing an AMOC reduction of 20% and 60% with respect to the control, respectively. This way, we could evaluate the impacts of a weak and strong AMOC reduction.

We have found that, due to a decreased northward ocean heat transport in the NH, a reduced AMOC leads to an average cooling over Europe and intensified cold extremes. However, despite the enhanced cooling, the frequency of cold spells (i.e. extremes with a duration of at least 6 days) is reduced. The mechanism we propose to explain this result is the following. During the boreal winter, the cooling at the NH's high latitudes intensifies the near-surface temperature meridional gradient. As a consequence, the jet stream intensifies and tends to stick around 45° N. An intensified jet stream reduces the frequency of atmospheric blocking systems in the North Atlantic and northwestern Europe. Since the North Atlantic blocking during winter is associated with prolonged periods of extreme cold temperatures in Europe, the cold spells there are also reduced. Interestingly, we have found that the change in the meridional temperature gradient due to the AMOC reduction is responsible for both a larger variability of *tasmin*, and therefore more intense extreme values, and a reduction of the persistent extreme cold events.

We decided to perform AMIP-like simulations to restrict the differences between the set of experiments to atmospheric variability only. A remaining question is to what extent our results are unaltered in coupled runs. In this sense, we repeated the analysis to the coupled run, finding very similar results (figure S6). In this case, the control run consists of 150 years of *piControl* (*ctrl*) to cover a complete multi-centennial AMOC variability reported by [41] and 60 years in which the AMOC strength is reduced by more than 50% with respect to the control (*hosing*). The results presented in this paper have the limitation of being extracted from a single model, the EC-Earth3 climate model. In this sense, more targeted experiments should be needed with other models to corroborate our results.

The relationship between atmospheric blocking in the NH and the occurrence of cold spells in Europe is widely studied. It has been reported that winters with increased blocking events are associated with extremely cold temperatures over central to Eastern Europe during the boreal winter (e.g. [42, 43]). Brunner *et al* [44] studied the relation between temperature extremes and the location of atmospheric blocking with the second generation of CanESM2, and they found that up to 70% of the cold spells in central Europe during winter coincide with a blocking anywhere between 60° W and 30° E. The cooling effect of blocking in winter has been explained by the horizontal advection of cold air from higher latitudes or cold land such as the Arctic and Russia [45, 46]. Besides, the clear sky conditions associated with blocking anticyclones can enhance the development of cold anomalies [47]. Finally, the peculiar persistence that characterises the blocking helps prolong the cold anomalies that are needed for the occurrence of a cold spell.

With anthropogenic climate change, we expect enhanced warming both in the tropical upper troposphere and over the Arctic. The former would increase the meridional temperature gradient, strengthening

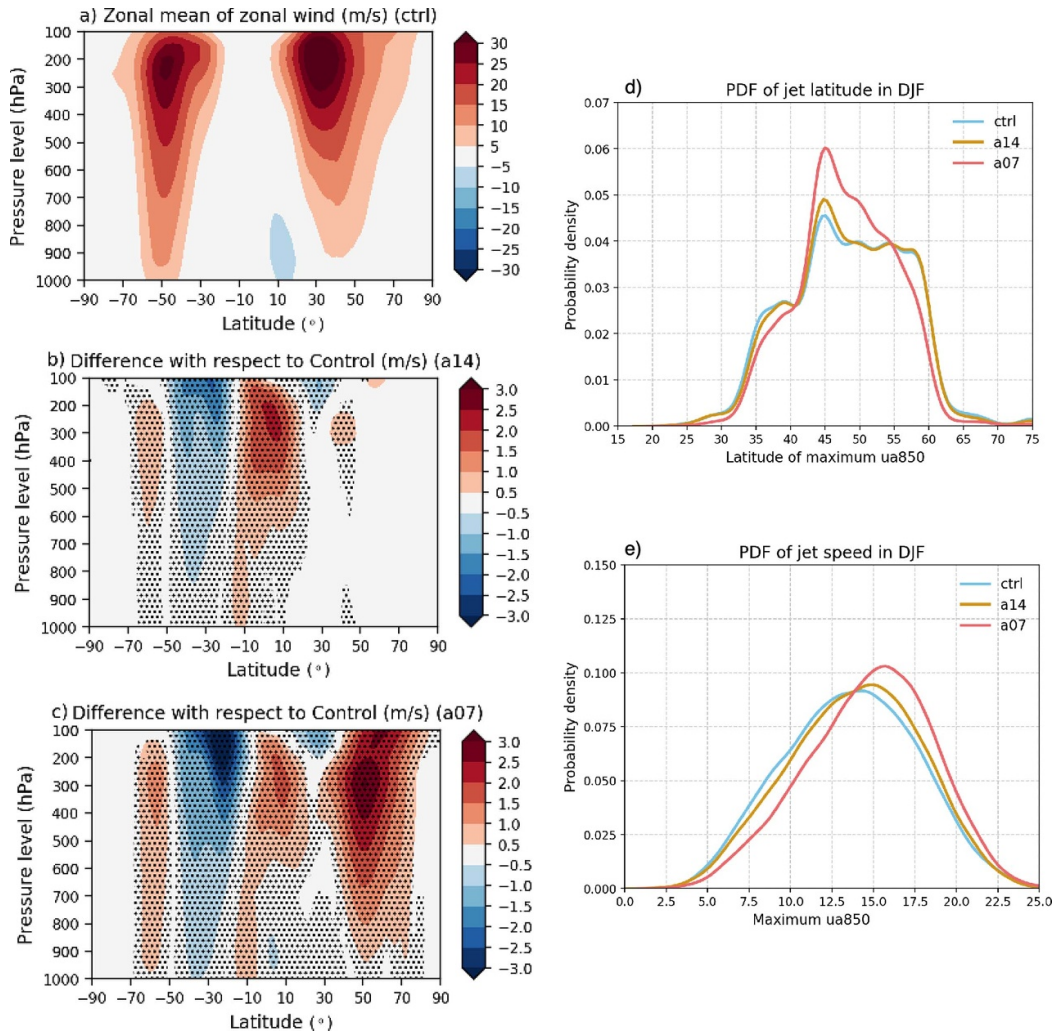

Figure 7. The jet stream. (a) shows the ensemble mean of the zonal wind as a function of latitude and pressure level for the *ctrl* experiments. (b) and (c) show the results for *a14* and *a07* as differences with respect to the control run. Dots are plotted when more than 75% of the ensemble members have the same sign of difference as the ensemble mean. (d) The daily jet-stream latitude index and (e) the daily jet-stream speed index for the three sets of experiments.

the jet stream and making it harder for blocks to form [48]. The latter, instead, would yield the opposite effect. Climate models currently suggest that upper tropospheric warming in the tropics will prevail. Consistently, CMIP3, CMIP5, and CMIP6 models project a decrease in blocking frequency in winter for the next decades [49]. In this sense, the effects of global warming and the impacts of a reduced AMOC act in the same direction, that is, a decrease of atmospheric blocking phenomenon in the North Atlantic. However, there is high uncertainty in current climate models in the amount of AMOC decline [50], which could have a significant influence on the cold spells and atmospheric blocking projections.

Data availability statement

The data that support the findings of this study are openly available at the following URL/DOI: https://doi.org/10.5281/zenodo.8391859 [51].

Acknowledgments

This is TiPES contribution #260. This work has received funding from the European Union's Horizon 2020 research and innovation program under Grant Agreement No. 820970 (TiPES) and from the Italian Ministry of Education, University and Research (MIUR) through the JPI Oceans and JPI Climate 'Next Generation Climate Science in Europe for Oceans'—ROADMAP Project (D. M. 593/2016). K B has received funding from the European Union's Horizon 2020 research and innovation programme under the Marie Sklodowska-Curie Grant Agreement No. 101026907 (CliMOC). The simulations used in this study have been carried out at ECMWF under the special Project SPITMEC2.

ORCID iDs

Virna L Meccia https://orcid.org/0000-0001-6905-2747

Claudia Simolo https://orcid.org/0000-0003-3634-1934
Katinka Bellomo https://orcid.org/0000-0001-7954-4390
Susanna Corti https://orcid.org/0000-0003-4456-6682

References

[1] Trenberth K E and Caron J M 2001 Estimates of meridional atmosphere and ocean heat transports *J. Clim.* **14** 3433–43
[2] Bjerknes J 1964 Atlantic air-sea interaction *Advances in Geophysics* vol 10 (Academic) pp 1–82
[3] Bryden H L and Imawaki S 2001 Ocean heat transport *Int. Geophys.* **77** 455–74
[4] Woollings T 2010 Dynamical influences on European climate: an uncertain future *Phil. Trans. R. Soc.* **368A** 3733–56
[5] Rahmstorf S, Box J E, Feulner G, Mann M E, Robinson A, Rutherford S and Schaffernicht E J 2015 Exceptional twentieth-century slowdown in Atlantic Ocean overturning circulation *Nat. Clim. Change* **5** 475–80
[6] Caesar A L, Rahmstorf S, Robinson A, Feulner G and Saba V 2018 Observed fingerprint of a weakening Atlantic Ocean overturning circulation *Nature* **556** 191–6
[7] Haarsma R J, Selten F M and Drijfhout S S 2015 Decelerating Atlantic meridional overturning circulation main cause of future west European summer atmospheric circulation changes *Environ. Res. Lett.* **10** 094007
[8] Lau N C and Ploshay J J 2013 Model projections of the changes in atmospheric circulation and surface climate over North America, the North Atlantic, and Europe in the twenty-first century *J. Clim.* **26** 9603–20
[9] Stouffer R J *et al* 2006 Investigating the causes of the response of the thermohaline circulation to past and future climate changes *J. Clim.* **19** 1365–87
[10] Vellinga M and Wood R 2008 Impacts of thermohaline circulation shut-down in the twenty-first century *Clim. Change* **91** 43–63
[11] Jackson L C, Kahana R, Graham T, Ringer M A, Woollings T, Mecking J V and Wood R A 2015 Global and European climate impacts of a slowdown of the AMOC in a high resolution GCM *Clim. Dyn.* **45** 3299–316
[12] Liu W, Fedorov A, Xie S-P and Hu S 2020 Climate impacts of a weakened Atlantic meridional overturning circulation in a warming climate *Sci. Adv.* **6** eaaz4876
[13] Zhang R and Delworth T L 2005 Simulated tropical response to a substantial weakening of the Atlantic thermohaline circulation *J. Clim.* **18** 1853–60
[14] Dahl K A, Broccoli A J and Stouffer R J 2005 Assessing the role of North Atlantic freshwater forcing in millennial scale climate variability: a tropical Atlantic perspective *Clim. Dyn.* **24** 325–46
[15] Bellomo K, Meccia V L, D'Agostino R, Fabiano F, Larson S M, Von Hardenberg J and Corti S 2023 Impacts of a weakened AMOC on precipitation over the Euro-Atlantic region in the EC-Earth3 climate model *Clim. Dyn.* **61** 3397–416
[16] Levermann A, Griesel A, Hofmann M, Montoya M and Rahmstorf S 2005 Dynamic sea level changes following changes in the thermohaline circulation *Clim. Dyn.* **24** 347–54
[17] Brayshaw D J, Woollings T and Vellinga M 2009 Tropical and extratropical responses of the North Atlantic atmospheric circulation to a sustained weakening of the MOC *J. Clim.* **22** 3146–55
[18] Jacob D, Goettel H, Jungclaus J, Muskulus M, Podzun R and Marotzke J 2005 Slowdown of the thermohaline circulation causes enhanced maritime climate influence and snow cover over Europe *Geophys. Res. Lett.* **32** L21
[19] Jendritzky G 1999 WMO/UNESCO sub-forum on science and technology in support of natural disaster reduction, chap *Impacts of Extreme and Persistent Temperatures—Cold Waves and Heat Waves* (World Meteorological Organization) pp 43–52 (available at: https://whycos.org/files/hwrp/wwd2004/docs/wmo914.pdf)
[20] Vajda A, Tuomenvirta H, Juga I, Nurmi P, Jokinen P and Rauhala J 2014 Severe weather affecting European transport systems: the identification, classification and frequencies of events *Nat. Hazards* **72** 169–88
[21] Añel J, Fernández-González M, Labandeira X, López-Otero X and de la Torre L 2017 Impact of cold waves and heat waves on the energy production sector *Atmosphere* **8** 209
[22] Döscher R *et al* 2022 The EC-Earth3 earth system model for the coupled model intercomparison project 6 *Geosci. Model Dev.* **15** 2973–3020
[23] ECMWF 2009 IFS cycle36r1 (European Center for Medium Range Forecast) (available at: www.ecmwf.int/en/publications/ifs-documentation) (Accessed 29 June 2023)
[24] Balsamo G, Beljaars A, Scipal K, Viterbo P, van den Hurk B, Hirschi M and Betts A K 2009 A revised hydrology for the ECMWF model: verification from field site to terrestrial water storage and impact in the integrated forecast system *Hydrometeorology* **10** 623–43
[25] Madec G 2008 NEMO ocean engine *Technical report* (Institut Pierre-Simon Laplace (IPSL))
[26] Vancoppenolle M, Fichefet T, Goosse H, Bouillon S, Madec G and Maqueda M A M 2009 Simulating the mass balance and salinity of Arctic and Antarctic sea ice. 1. Model description and validation *Ocean Model.* **27** 33–53
[27] Valcke S 2013 The OASIS3 coupler: a European climate modelling community software *Geosci. Model Dev.* **6** 373–88
[28] Jackson L C *et al* 2023 Understanding AMOC stability: the North Atlantic hosing model intercomparison project *Geosci. Model Dev.* **16** 1975–95
[29] Zhang X B, Alexander L, Hegerl G C, Jones P, Tank A K, Peterson T C, Trewin B and Zwiers F W 2011 Indices for monitoring changes in extremes based on daily temperature and precipitation data *Wiley Interdiscip. Rev.-Clim. Change* **2** 851–70
[30] Davini P 2018 MiLES—mid latitude evaluation system (version v0.51) *Zenodo* https://doi.org/10.5281/zenodo.1237838
[31] Davini P, Cagnazzo C, Gualdi S and Navarra A 2012 Bidimensional diagnostics, variability, and trends of Northern Hemisphere blocking *J. Clim.* **25** 6496–509
[32] Woollings T, Czuchnicki C and Franzke C 2014 Twentieth century North Atlantic jet variability *Q. J. R. Meteorol. Soc.* **140** 783–91
[33] Delworth T L, Cooke W F, Naik V, Paynter D J and Zhang L 2022 A weakened AMOC may prolong greenhouse gas–induced Mediterranean drying even with significant and rapid climate change mitigation *Proc. Natl Acad. Sci.* **119** e2116655119
[34] Simolo C and Corti S 2022 Quantifying the role of variability in future intensification of heat extremes *Nat. Commun.* **13** 7930
[35] Holmes C R, Woollings T, Hawkins E and de Vries H 2016 Robust future changes in temperature variability under greenhouse gas forcing and the relationship with thermal advection *J. Clim.* **29** 2221–36
[36] Tamarin-Brodsky T, Hodges K, Hoskins B J and Shepherd T 2020 Changes in Northern Hemisphere temperature variability shaped by regional warming patterns *Nat. Geosci.* **13** 414–21
[37] Corti S, Giannini A, Tibaldi S and Molteni F 1997 Patterns of low-frequency variability in a three-level quasi-geostrophic model *Clim. Dyn.* **13** 883–904
[38] Madonna E, Li C, Grams C M and Woollings T 2017 The link between eddy-driven jet variability and weather regimes

in the North Atlantic-European sector *Q. J. R. Meteorol. Soc.* **143** 2960–72
[39] Fabiano F, Meccia V L, Davini P, Ghinassi P and Corti S 2021 A regime view of future atmospheric circulation changes in northern mid-latitudes *Weather Clim. Dyn.* **2** 163–80
[40] Nakamura N and Huang C S Y 2018 Atmospheric blocking as a traffic jam in the jet stream *Science* **361** 42–47
[41] Meccia V L, Fuentes-Franco R, Davini P, Bellomo K, Fabiano F, Yang S and von Hardenberg J 2022 Internal multi-centennial variability of the Atlantic Meridional Overturning Circulation simulated by EC-Earth3 *Clim. Dyn.* **60** 3695–712
[42] Buehler T, Raible C C and Stocker T F 2011 The relationship of winter season North Atlantic blocking frequencies to extreme cold or dry spells in the ERA-40 *Tellus* A **63** 212–22
[43] Sillmann J, Croci-Maspoli M, Kallache M and Katz R W 2011 Extreme cold winter temperatures in Europe under the influence of North Atlantic atmospheric blocking *J. Clim.* **24** 5899–913
[44] Brunner L, Schaller N, Anstey J, Sillmann J and Steiner A K 2018 Dependence of present and future European temperature extremes on the location of atmospheric blocking *Geophys. Res. Lett.* **45** 6311–20
[45] Bieli M, Pfahl S and Wernli H 2015 A lagrangian investigation of hot and cold temperature extremes in Europe *Q. J. R. Meteorol. Soc.* **141** 98–108
[46] Sousa P M, Trigo R M, Barriopedro D, Soares P M M and Santos J A 2018 European temperature responses to blocking and ridge regional patterns *Clim. Dyn.* **50** 457–77
[47] Trigo R M, Trigo I F, DaCamara C C and Osborn T J 2004 Climate impact of the European winter blocking episodes from the NCEP/NCAR Reanalyses *Clim. Dyn.* **23** 17–28
[48] Woollings T, Barriopedro D, Methven J, Son S-W, Martius O, Harvey B, Sillmann J, Lupo A R and Seneviratne S 2018 Blocking and its response to climate change *Curr. Clim. Change Rep.* **4** 287–300
[49] Davini P *et al* 2020 From CMIP3 to CMIP6: Northern Hemisphere atmospheric blocking simulation in present and future climate *J. Clim.* **33** 10021–38
[50] Bellomo K, Angeloni M, Corti S and Von Hardenberg J 2021 Future climate change shaped by inter-model differences in Atlantic meridional overturning circulation response *Nat. Commun.* **12** 3659
[51] Meccia V, Simolo C, Bellomo K and Corti S 2023 Extreme cold events in Europe under a reduced AMOC *Zenodo* https://doi.org/10.5281/zenodo.8391859